



Travertine increases the concentration of trace elements in groundwater in Chahar Takab, Fariman county, northeast Iran

Maryam Rezanezhad^{1,2} · Mohamad Hosein Mahmudy-Gharaie² · Nicola Fohrer¹ · Daniel Rosado^{1,3}

Received: 16 November 2024 / Accepted: 9 February 2025 / Published online: 20 February 2025
© The Author(s) 2025

Abstract

Groundwater has emerged as a crucial water source, supplying half of the world's domestic water needs, particularly in rural areas without supply systems. This study assesses the impact of travertine formations, on water quality in Chahar Takab village, Iran, focusing on suitability for human consumption and ecosystem sustainability where groundwater is the primary source. Thirty-four samples from various sources, including travertine springs, surface water, and groundwater, underwent ICP-OES analysis. Travertine springs exhibited higher electrical conductivity (EC), lower pH, and elevated concentrations of major cations (Na, Ca, Mg) and anions (Cl, HCO₃). In them, all samples exceeded European Union limits for Cl and Na in drinking water. Hydrochemical facies were influenced by water-rock interactions, leading to Ca-HCO₃ dominance in surface and groundwater samples and Ca-Mg-Cl dominance in travertine springs. Heavy metal analysis revealed high concentrations of As, B, Fe, Mn, and Pb in travertine spring and surface water samples, with As exceeding World Health Organization limits by up to 28.5 times. Additionally, the Metal Index indicated values exceeding drinking water guidelines set by the World Health Organization in 58% of the samples. Travertine springs had the highest toxicity risks, especially for As, Cd, and Pb. Results suggest a tectonic origin for heavy metal contamination (As-containing travertine springs), emphasizing the need for mitigation measures and regular monitoring. Action is necessary to address water quality issues in the region.

Highlights

- Travertine reduces groundwater quality.
- Ca-HCO₃ dominates surface and groundwater.
- Ca-Mg-Cl dominantes in travertine springs.
- High concentrations of As, B, Fe, Mn, and Pb.
- Toxicity risks associated with As, Cd, and Pb.

Keywords Groundwater quality · Arsenic · Heavy metal pollution · Drinking water · Travertine springs · Water scarcity

Introduction

Two billion people worldwide lack access to safe drinking water (United and Nations 2022). Furthermore, half of the global population experiences severe water scarcity for at least part of the year (IPCC 2022). This situation is projected to intensify in the future due to climate change and population growth (World Meteorological and Organization 2022). Consequently, groundwater has become a vital water source, supplying half of the world's domestic water needs (UNESCO World Water Assessment Programme 2022). In rural areas without supply systems, it often serves as the only viable option for providing basic water access (UNESCO

✉ Daniel Rosado
drosado@hydrology.uni-kiel.de

¹ Department of Hydrology and Water Resources Management, Institute for Natural Resource Conservation, Kiel University, Kiel 24118, Germany

² Department of Geology, Faculty of Science, Ferdowsi University of Mashhad, Mashhad, Iran

³ Department of Chemical and Environmental Engineering, Universidad de Sevilla, Camino de los Descubrimientos, s/n, Sevilla 41092, Spain

World Water Assessment Programme 2022). Remarkably, the Asia-Pacific region leads global groundwater extraction, with seven of the top ten groundwater-extracting nations (Bangladesh, China, India, Indonesia, Iran, Pakistan and Turkey) accounting for approximately 60% of the world's total groundwater withdrawal (UNESCO World Water Assessment Programme 2022).

Although groundwater resources are often abundant, their quality can be affected by industries, mining, urban effluents and other anthropogenic activities, as well as natural factors such as specific lithologies or the presence of travertine springs (Kumar et al. 2019; Vardhan et al. 2019). The chemical interactions between groundwater and minerals, known as hydrogeochemical processes, that involve mineral dissolution and precipitation, ion exchange, oxidation-reduction reactions, and adsorption-desorption mechanisms, together with the geological characteristics of an area, such as rock type, mineral composition, and structural features, largely influence the physicochemical characteristics of groundwater (Aju et al. 2022; Islam 2023).

The so-called heavy metal (i.e. trace elements) are frequent pollutants of groundwater and their presence has become a global issue with potential adverse impacts on human health (Amaral et al. 2018; He and Wu 2019a, b; Masoudinejad et al. 2018). Groundwater is particularly affected by non-anthropogenic elements such as As, F, Cr, B, and others, which originate from geological formations, water-rock ion exchange, and degassing of magma intrusion (Delkhahi et al. 2020).

Among the mentioned heavy metals, especially inorganic As pollution in groundwater resources became a global challenge (Roh et al. 2017). Inorganic As constitutes the main form of As found in groundwater, surface water, and soil (Pazhoor et al. 2021). It can be present in water as Arsenite, As (III), the most toxic form of As, and as Arsenate, As (V), less toxic (Biswas et al. 2019; Chakraborti et al. 2016). The primary source of inorganic As in groundwater is geological weathering, but also anthropogenic sources can be involved (Biswas and Sarkar 2019). As has been categorized as a Group A carcinogen, denoting it as a 'known' human carcinogen, by both the United States Environmental Protection Agency (USEPA 2004) and the International Agency for Research on Cancer (American Cancer Society 2020). This classification is based on the chronic toxicity effects of As in drinking water. To mitigate this risk, the World Health Organization (WHO) lowered the permissible limit for As in drinking water to 10 µg/l (Foster et al. 2019). Usually, As concentrations in uncontaminated surface water ranges from 1 to 10 µg/l. However, in mining and mineralization areas, these levels can significantly escalate (Kumar et al. 2019). Travertine rock is a unique type of limestone formed by the deposition of CaCO₃ from hydrothermal

vents along fractures and faults in the Earth's crust (Grootjans et al. 2015; Henchiri et al. 2017; Kano et al. 2019; Pola et al. 2014; Shiraishi et al. 2020). Travertine is a sedimentary freshwater carbonate rock that forms from hydrothermal water springs rich in Ca²⁺ and with high partial pressure of CO₂ (Kano et al. 2019). When this water emerges at the surface, rapid CO₂ degassing occurs, increasing pH and triggering the precipitation of CaCO₃ according to the reaction: $\text{Ca}^{2+} + 2\text{HCO}_3^- \leftrightarrow \text{CaCO}_3 + \text{CO}_2 + \text{H}_2\text{O}$ (Kano et al. 2019). Typically, travertine formation involves CO₂ and fluids of deep origin (Janssens et al. 2020). In contrast, tufa, another freshwater carbonate, forms in cool, ambient temperature freshwater environments through biologically induced processes and often contains remnants of micro- and macrophytes, invertebrates, and bacteria (Kele and Bódoi 2022). Additionally, tufa forms from shallow CO₂ sources, such as soil biodegradation or plants (Janssens et al. 2020).

Travertine springs waters are frequently rich in various elements, including potentially high levels of trace elements, due to the travertine rock-water interaction in deep aquifers (Durowoju et al. 2015). This process can directly reduce the quality of surface and groundwater or cause alterations through infiltration, discharge-recharge pattern of groundwater, inter-aquifer exchange, etc. Consequently, it can hinder the suitability of these waters for drinking and agricultural purposes (Kampouroglou and Economou-Eliopoulos 2016; Rezaei et al. 2018).

The effects of travertine spring waters on trace elements, especially As, have attracted attention of researchers worldwide (Kano et al. 2019; Rezaei et al. 2018). Geothermal areas in Japan and locations with thermal activity in New Zealand have reported exceptionally high As concentrations in water, reaching 6400 µg/l and 8500 µg/l, respectively (Shakeri et al. 2020). Therefore, studies investigating As contamination have been conducted worldwide, including the United States, China, Argentina, Chile, Bolivia, Peru, Mexico, Bangladesh, Japan, India, Nepal, among others (Ayotte et al. 2015; Bhowmick et al. 2018; He et al. 2020; Hossain et al. 2016; Huq et al. 2020; Mueller 2017; Ortega-Guerrero 2017; Tapia et al. 2019) and has recently been reported in Iran (Mohammadzadeh and Mansouri Daneshvar, 2020).

In the Fariman area, northeast Iran, numerous travertine springs align with fault and fracture trends, often corresponding to inner faults. Over time, travertine springs have led to the leaching of toxic elements from alteration zones into local water sources. Given the extensive distribution of travertine springs in Chahar Takab village, their alignment with faults, and the significant human population relying on these waters for drinking, agriculture, and other purposes, we aim to assess the impact of travertine formations and the regional geology on major and minor components in water

and, therefore, their suitability for both human consumption and sustaining aquatic ecosystems within the catchment area. This objective aligns with the concerns highlighted in the United Nations World Water Development Report 2022 regarding the lack of reliable data for area-specific groundwater assessments to enable informed policies and groundwater resources management.

Materials and methods

Study area

The study area lies between latitude 35°20' to 35°34' N and longitude 59°53' to 60°04' E. It includes Chahar Takab (35°29'56.8"N 59°53'15.6"E), a rural village located in Fariman county, Razavi Khorasan province (northeast Iran), 25 km south of Fariman city and 115 km southeast of Mashhad city (Fig. 1). The study area has a BSk climate according to the Köppen climate classification (World Bank 2021). Fariman city experiences cold and long winters. In the coldest months (December and January) temperature can drop

to -17 °C while in the hottest (July and August) can reach 36 °C (Iran Data Portal 2022). Annual rainfall is in the range of 150 to 200 mm (Iran Data Portal 2022).

The study area lacks Paleocene and Oligocene facies. The oldest geological unit dates back to the Precambrian period and consists of a sequence of metamorphic rocks (Iran Oil and Company 1957). Near Chahar Takab village, a Miocene rock formation is present, characterized by layers of clay or siltstone interbedded with conglomerate, along with limestone layers to the southeast (Iran Oil and Company 1957). A geological map with data of the United States Geological Survey is in the supplementary material (Figure S1).

In-situ parameters and water sampling

In-situ parameters were measured, and water samples were collected from 34 sampling points in July 2019. In situ parameters included pH, electrical conductivity (EC) and temperature. Two bottles of water (500 ml) were collected at each point. Each bottle was washed three times with local water prior to water collection and no air bubbles were allowed in the bottles after collection. Due to the limited

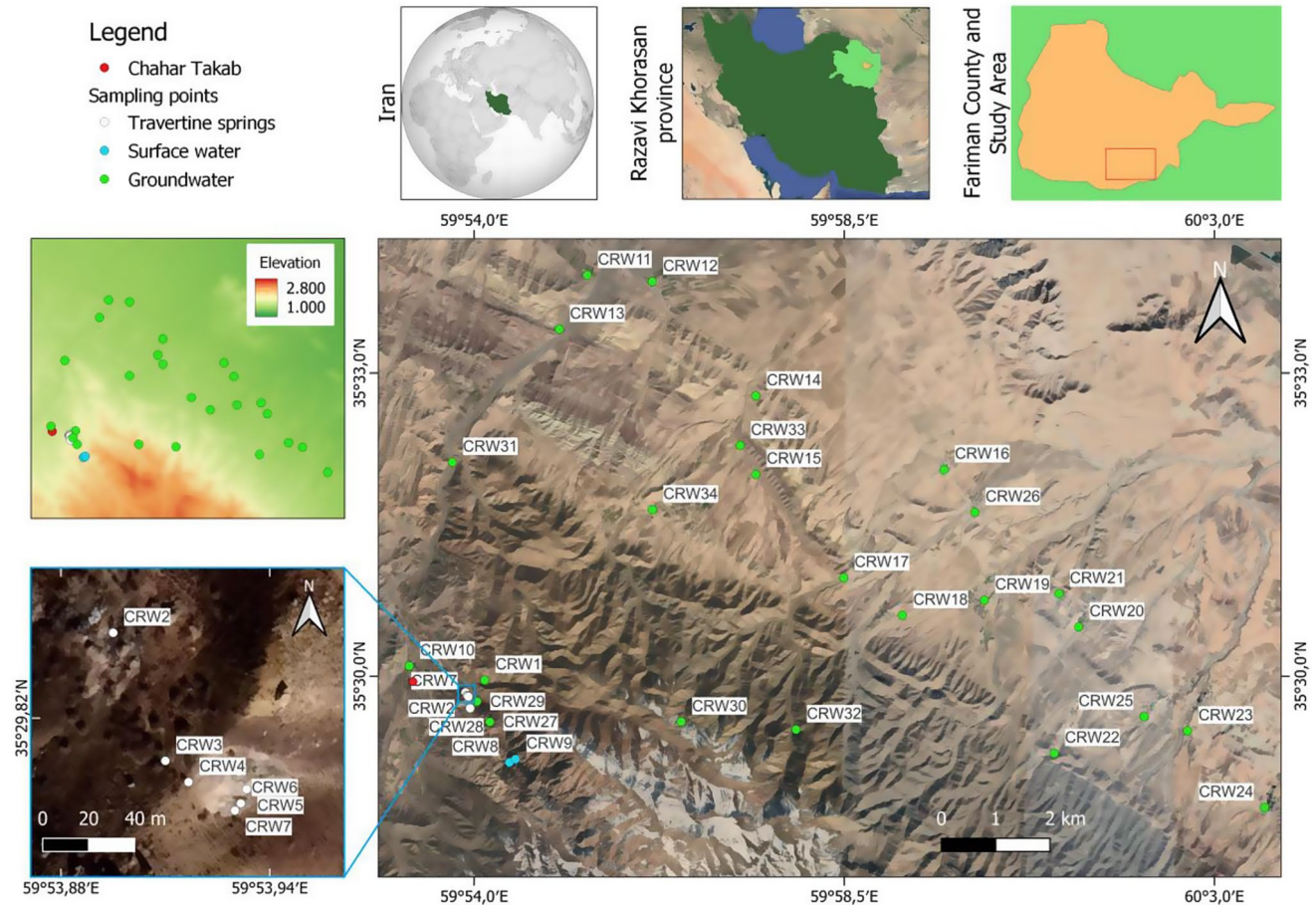


Fig. 1 Location of the water sampling points

water resources in travertine springs, samples were collected there with a syringe.

The points were categorized into three groups, as detailed in Table 1. Group 1 comprised samples from travertine springs located at high altitudes (average: 1776 m.a.s.l.). Group 2 consisted of surface water collected at the highest locations (1827 and 1957 m.a.s.l.). Group 3 involved various types of groundwater samples: springs, well water, and groundwater transported in aqueducts. Group 3 samples were collected at lower altitudes (average: 1578 m.a.s.l.), except for CRW1, CRW27, CRW30 and CRW32, which were collected at higher altitudes (1754 to 2097 m.a.s.l.).

Laboratory analysis

Samples were transported to the Central Laboratory of Ferdowsi University in Mashhad, Iran, where all laboratory analysis were conducted. To prevent any reaction with

oxygen, carbonate (CO_3^{2-}), bicarbonate (HCO_3^-) and total alkalinity (T) were measured immediately after sampling using the titration method with phenolphthalein and methyl orange, following ISO 9963-1:1996. Sulfate (SO_4^{2-}) was measured with a spectrophotometer (DU-6 Spectrophotometer, 420 nm; BECKMAN) at 420 nm following Standard Methods 4500-SO₄²⁻ E with barium chloride (BaCl_2) and other reagents. Chloride (Cl^-) was determined by titration with silver nitrate (AgNO_3) and potassium chromate (K_2CrO_4 5%) following Standard Methods 4500-Cl- B. Ca and Mg, were analyzed by titration with EDTA according to Standard Methods 3500-Ca B and Standard Methods 3500-Mg B. To analyze As and the rest of the metals, 100 ml of collected water samples were filtered (0.25 μm) and acidified to $\text{pH} < 2$ with nitric acid to prevent metal oxidation (Ghosh et al. 2019). Potassium (K) and Sodium (Na) as well as As, Cd, Cr, Co, Pb, Mn, Ni, Zn were determined with an ICP-OES (76004555 SPECTRO ARCOS System).

Table 1 Coordinates and altitude of the sampling points

Group	Point	Latitude (North)	Longitude (East)	Altitude (masl)	Source of water
1 - Travertine springs	CRW2	35° 29' 50.4"	59° 53' 53.7"	1761	Travertine spring (1)
	CRW3	35° 29' 48.6"	59° 53' 54.6"	1779	Travertine spring (2)
	CRW4	35° 29' 48.3"	59° 53' 55.0"	1783	Travertine spring (3)
	CRW5	35° 29' 48.2"	59° 53' 56.0"	1772	Travertine spring (4)
	CRW6	35° 29' 48"	59° 53' 55.9"	1794	Travertine spring (5)
	CRW7	35° 29' 47.9"	59° 53' 55.8"	1785	Travertine spring (6)
	CRW28	35° 29' 41"	59° 53' 57.0"	1761	Travertine spring (7)
2 - Surface water	CRW8	35° 29' 8.8"	59° 54' 25.7"	1827	River water
	CRW9	35° 29' 10.7"	59° 54' 30.1"	1911	Waterfall
3 - Ground water	CRW1	35° 29' 57.7"	59° 54' 7.7"	1754	Chahar Takab spring
	CRW10	35° 30' 6.2"	59° 53' 12.6"	1686	Drinking water
	CRW11	35° 33' 58.2"	59° 55' 22.5"	1502	Golesheikh village aqueduct
	CRW12	35° 33' 54.4"	59° 56' 9.9"	1488	Golesheikh village well
	CRW13	35° 33' 26.1"	59° 55' 2.1"	1502	Kalate Rostam aqueduct
	CRW14	35° 32' 46.5"	59° 57' 25.4"	1620	Mazare Bi Abe aqueduct
	CRW15	35° 32' 0"	59° 57' 25.4"	1460	Taraz Khaki village spring
	CRW16	35° 32' 2.7"	59° 59' 42.7"	1444	Taraz Khaki village aqueduct
	CRW17	35° 30' 58.6"	59° 58' 29.5"	1553	Golestan village aqueduct
	CRW18	35° 30' 36.3"	59° 59' 12.3"	1549	Kariz Balagh village aqueduct
	CRW19	35° 30' 45.2"	60° 0' 12.2"	1461	Kariz Balagh village spring
	CRW20	35° 30' 29.3"	60° 1' 20.9"	1460	Galayem aqueduct
	CRW21	35° 30' 49.1"	60° 1' 6.5"	1439	Heidar spring of Galayem village
	CRW22	35° 29' 14.2"	60° 1' 3.1"	1569	Chaharbid aqueduct
	CRW23	35° 29' 27.6"	60° 2' 40.4"	1461	Kariz Sokhte aqueduct (1)
	CRW24	35° 28' 42"	60° 3' 36.6"	1429	Chenarbo aqueduct
	CRW25	35° 29' 36"	60° 2' 8.7"	1451	Kariz Sokhte aqueduct (2)
	CRW26	35° 31' 37.5"	60° 0' 5.2"	1448	Kariz Balagh aqueduct
	CRW27	35° 29' 32.9"	59° 54' 11.4"	1815	Spring surrounding the travertine springs
	CRW29	35° 29' 45"	59° 54' 2.0"	1737	Spring surrounding the travertine
	CRW30	35° 29' 33"	59° 56' 31.0"	2097	Aqueduct in front of Golesheikh village
	CRW31	35° 32' 7"	59° 53' 44.0"	1575	aqueduct in front of Mazare Bi Abe
	CRW32	35° 29' 28.3"	59° 57' 54.8"	1955	Spring surrounding Golestan village
	CRW33	35° 32' 17"	59° 57' 14.0"	1468	Spring before Mazare Bi Abe village
	CRW34	35° 31' 39"	59° 56' 10.0"	1530	Estakhr village aqueduct

Hydrochemical facies and Piper diagrams

The concentrations of the major cations (Na^+ , K^+ , Ca^{2+} , Mg^{2+}) and major anions (HCO_3^- , CO_3^{2-} , SO_4^{2-} , Cl^-) were used to determine the hydrochemical characteristics of water samples. These data were represented in a Piper diagram using D-Piper software (Moreno Merino et al. 2021). Piper diagrams classify water into 6 ranges or types: first type (calcium bicarbonate water, Ca- HCO_3), second type (sodium chloride, Na-Cl), third type (calcium magnesium chloride, Ca-Mg-Cl), fourth type (calcium bicarbonate sodium, Ca-Na- HCO_3), fifth type (calcium chloride, Ca-Cl) and sixth type (sodium bicarbonate, Na- HCO_3).

The Piper diagram shows water type, ion exchange, element dissolution or deposition, as well as mixing with other waters (Hounslow 2018; Shakoor et al. 2018).

Pearson correlation coefficient

Pearson correlation coefficients for major cations and anions, pH and EC in groundwater were calculated using SPSS software. Correlation analysis provides valuable insights into ions with common origins, as well as those contributing significantly to pH and EC levels in the water (Yousefi et al. 2018).

Metal Index (MI)

Metal Index (MI) introduced by Tamasi and Cini (2004) was calculated using trace elements data using the following formula.

$$MI = \sum_{i=1}^n \frac{Cf}{(MAC)_i}$$

where Cf is the concentration of each element in water, MAC is the maximum allowable concentration for a metal element based on drinking water guidelines from various sources, including the World Health Organization (WHO 2022): As (10 $\mu\text{g/l}$), B (2400 $\mu\text{g/l}$), Cd (3 $\mu\text{g/l}$), Cr (50 $\mu\text{g/l}$), Cu (2000 $\mu\text{g/l}$), Mn (80 $\mu\text{g/l}$), Ni (70 $\mu\text{g/l}$), Pb (10 $\mu\text{g/l}$), Se (40 $\mu\text{g/l}$); the European Union (European Parliament 2020): Fe (200 $\mu\text{g/l}$); and the USEPA (USEPA 2022): Zn (5000 $\mu\text{g/l}$). Finally, i represents the ith sample. A higher metal index value indicates a higher concentration of metals relative to the allowable limit and, therefore, lower water quality. If the concentration of a particular element is higher than the allowable limit ($MI > 1$), the water is considered contaminated for that element. Conversely, if the concentration of an element is lower than the allowable limit ($MI < 1$), the water is considered free of contamination by that element.

Results and discussion

In situ parameters

Temperature, pH and conductivity values are presented in Fig. 2 and all the values are compiled in the supplementary material (Table S1). Results have been categorized into three groups based on water type, as shown in Table 1. Temperature in group 1 displayed the highest mean (average 22.4°C, range 17.5–28.5°C) compared to group 2 (average 15°C, range 14.5–15.5°C) and group 3 (average 18.5°C, range 14.5–25.5°C). pH exhibited a lower average within travertine springs of group 1 (average 6.94, range 6.17–7.66) compared to groups 2 (average 8.31, range 8.28–8.33) and 3 (average 7.93, range 7.26–8.92). Regarding conductivity, higher values were observed in the travertine springs of group 1 (average 8733 $\mu\text{S/cm}$, range 4780–12360 $\mu\text{S/cm}$) compared to surface water of group 2 (average 419 $\mu\text{S/cm}$, range 408–430 $\mu\text{S/cm}$) and groundwater of group 3 (average 1273 $\mu\text{S/cm}$, range 560–4850 $\mu\text{S/cm}$). Sample 28 displayed some differences with other samples of group 1, including the lowest conductivity in this group, probably because was distant from the rest.

Results indicated that pH is lower and dissolved salts are higher in travertine springs, a characteristic attributed to their geothermal origins (Kano et al. 2019). These springs originate from groundwater that permeates limestone-rich geological formations, becoming enriched in Ca^{2+} and HCO_3^- through the dissolution of CaCO_3 by CO_2 present in the water (Hielt et al. 2022; Luo et al. 2022). As water emerges from the springs, changes in pressure and temperature lead to CO_2 degassing, reducing the solubility of calcium carbonate and precipitating dissolved ions in the surrounding areas (Brilli and Giustini 2023; Gao et al. 2023; Ranjbaran and Zamanzadeh 2021; Wang et al. 2015). Travertine springs interestingly exemplify groundwater geochemistry influenced by the interaction between alkalinity and dissolved CO_2 (Brilli and Giustini 2023; Ranjbaran and Zamanzadeh 2021). The process of CO_2 uptake by water at depth and its release at the surface not only regulates pH and alkalinity but also drives the continuous formation and growth of travertine deposits around the spring.

None of the samples of group 1 meet the drinkability criteria set by the European Union (European Parliament 2020). Specifically, all the samples within this group surpass the established conductivity limit of 2500 $\mu\text{S/cm}$, and additionally, CRW2, CRW3, and CRW4 samples fall below the lower pH threshold within the prescribed range of 6.5–9.5. Conversely, the conductivities of samples in groups 2 and 3 remained below this limit.

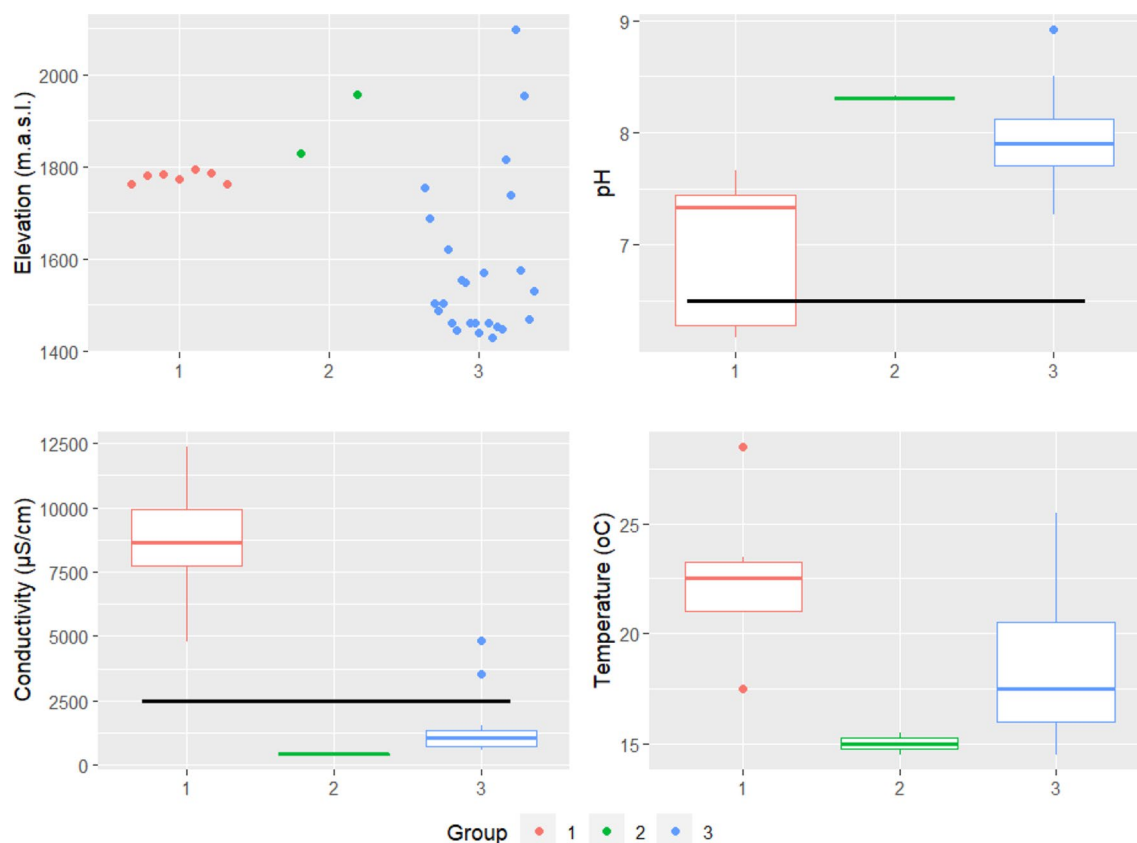


Fig. 2 Elevation, temperature, pH and electrical conductivity in three groups of water samples (group 1, travertine springs, red; group 2, surface water, green; group 3, groundwater, blue) collected in Cha-

har Takab, Fariman county, northeast Iran along with drinking water thresholds for pH (6.5) and conductivity (2500 µS/cm) set by the European Union (European Parliament 2020)

Concentrations of the major cations (Na^+ , K^+ , Ca^{2+} , Mg^{2+}) and major anions (HCO_3^- , CO_3^{2-} , SO_4^{2-} , Cl^-)

As detailed in the supplementary material (Table S1), the predominant anion in group 1 samples was Cl^- (average 1462 mg/l, range 504–2190 mg/l), followed by HCO_3^- (average 1002 mg/l, range 622–1391 mg/l) while in groups 2 and 3, HCO_3^- was the predominant anion (averages 198 and 309 mg/l, ranges 195–201 and 238–421 mg/l, respectively). Among cations, Na showed the highest concentrations (average 1200 mg/l, range 435–1808 mg/l) in group 1. Group 2 presented similar levels of Ca (average 70 mg/l) and Mg (average 100 mg/l), while in group 3, Mg exhibited the highest concentration (average 254 mg/l, range 90–790 mg/l).

The European Union and the USEPA set a limit of 250 mg/l Cl^- and 200 mg/l Na in drinking water (European Parliament 2020; USEPA 2023, 2022). All group 1 samples and some in group 3 exceeded these limits and therefore, are unsuitable for drinking, while all groups 2 samples remained within the permissible range.

Defining thresholds for Ca and Mg in drinking water remains a challenge. Several researchers have proposed

that minimum levels of approximately 20 to 30 mg/l Ca and 10 mg/l Mg in drinking water could yield health benefits, including reduced cardiovascular mortality (WHO 2005). The World Health Organization also indicate that the taste threshold for Ca ions falls within the range of 100–300 mg/l, depending on the associated anion, and suggests that the taste threshold for Mg is probably lower than that for Ca (WHO 2022). In the case of Ca, all the samples in group 1 and some in group 3 are above these limits indicating suboptimal characteristics for drinking water. In the case of Mg, samples in group 1 well exceed the threshold, as well as most of the samples of groups 2 and 3.

Elevated Na in groundwater and springs is often attributed to the weathering of plagioclases, which have a high Na content, such as albite in igneous rocks. Also, to other Na-containing silicate minerals, such as nepheline, part of the feldspathoid group and present in igneous rocks. Furthermore, the presence of minerals such as halite and mirabilite in evaporitic rocks has also been associated with increased Na concentrations (Nugraheni and Sunjaya 2019). In the study area, high Na concentrations exhibit a strong correlation with Cl ($R^2=0.8$) in group 1 samples, with a slope of 1.1. This slope is close to the 1:1 ratio typically associated

with halite weathering, suggesting that halite dissolution is likely the primary source of these elevated ion concentrations (Zhang et al. 2020).

Sulfates concentrations were higher in group 1 (average 33.1 mg/l, range 14.4–55.3 mg/l) and lower in group 3 (average 13.3 mg/l, range 0.02–48.5 mg/l) and group 2 (average 0.12 mg/l, range 0.08–0.16 mg/l). All measured samples fell below the World Health Organization limit of 250 mg/l for sulfates in drinking water. Similar to Ca and Mg, this limit serves as a guideline for public acceptability and taste detection rather than as a health-based guideline (WHO 2022). The predominant source of SO_4^{2-} has been associated with reactions of water and travertine rock (Hamidian et al. 2019). These results show an increase on sulfate concentrations in group 1 samples, where travertine is present, while the baseline sulfate concentration in group 3 samples remain relatively low. This difference is likely attributed to the reduced presence of sulfate-bearing minerals in the geological formations of group 3 areas. Concerning bicarbonates, travertine spring waters of group 1 exhibited elevated levels of HCO_3^- (average 1002 mg/l, range 622–1391 mg/l) due to limestones decomposition (Kano et al. 2019) compared to group 2 (average 198 mg/l, range 195–201 mg/l) and group 3 (average 309 mg/l, range 238–421 mg/l). This concentration in group 1 was likely different when the water was still underground. When groundwater rises to the surface, CO_2 dissolved in water evaporates because of the new equilibrium with the very low CO_2 content of the air, therefore, the pH increases, bicarbonate decreases and carbonate increases (Ulloa-Cedamano et al. 2020). If calcium ions were present in water, both would precipitate as CaCO_3 (Ulloa-Cedamano et al. 2020).

Based on the geological units displayed in the map in Figure S1, i.e. Q: Quaternary; Pg: Paleogene; Pz: Paleozoic; K: Cretaceous, unit K shows higher concentrations of all ions, lower pH, and higher EC. These values are attributed to the presence of travertine springs within this unit. In contrast, no significant differences are observed between units Pg and Pz, except for Na and Cl, which are higher in Pg compared to Pz.

Hydrochemical facies and Piper diagrams

The piper diagram (Piper 1944) is depicted in Fig. 3. In the present study, group 1 samples belong to third type (calcium magnesium chloride, Ca-Mg-Cl). Group 2 samples are classified as the first type (calcium bicarbonate water, Ca- HCO_3). Within group 3, most samples align with the first type, although one sample aligns with the third type (calcium magnesium chloride, Ca-Mg-Cl), and another with the fourth type (calcium bicarbonate sodium, Ca-Na- HCO_3).

The lithology and mineralogy of the aquifer determines the hydrochemical facies type found in the groundwater. The predominance of calcium bicarbonate (Ca- HCO_3) in group 2 and 3 indicates the dissolution of calcite and carbonate rocks. In the travertine springs of group 1, the abundance of Ca and Mg ions indicates a large ion exchange process.

Pearson correlation coefficient

Pearson correlation coefficients are presented in Table 2. The significant relationships among pH, EC and HCO_3^- can be attributed to the close contact between travertine spring water and CaCO_3 . Consequently, these waters exhibit higher level of EC and HCO_3^- , and also a lower pH due to the contact with CO_2 (Luo et al. 2022). EC displays a positive and very strong correlation with all the main anions and cations, except CO_3^{2-} , which is explained by the dependence of EC on dissolved ions.

A strong positive correlation is observed between HCO_3^- and Na, particularly in group 1. This aligns with the findings of Guettaf et al. (2017), who noted that elevated HCO_3^- in water increases the deposition of CaCO_3 and MgCO_3 , and therefore proportionally increases concentrations of Na. Moreover, As and sulfate have a positive and significant correlation, suggesting their concurrent release into the water. Thus, As and B can be linked to the oxidation of sulfide minerals in regenerative mineralization, in addition to travertine sources.

Heavy metals analysis and Metal Index (MI)

The results of the heavy metal analysis are depicted in Fig. 4 and detailed in the supplementary material (Table S2). Group 1 samples showed the highest metal concentration averages in the cases of As, B, Cd, Cu, Fe, Mn, Zn and Se.

The average concentrations of several elements in groups 1, 2 and 3 surpassed the drinking water standards established by the World Health Organization (WHO 2022). Specifically, the average concentrations of As in groups 1 and 2 (285 $\mu\text{g/l}$; 15.4 $\mu\text{g/l}$), B in group 1 (21660 $\mu\text{g/l}$), Fe in groups 1 and 3 (680 $\mu\text{g/l}$; 176 $\mu\text{g/l}$), Mn in group 1 (215 $\mu\text{g/l}$) and Pb in group 1 (12.1 $\mu\text{g/l}$). Furthermore, several individual samples exhibited metal concentrations that exceeded the mentioned standards, as indicated in Fig. 4. On the contrary, the average values of Cd, Cr, Cu, Mn, Ni, Zn, and Se, were lower.

Notably, As concentrations in group 1 samples were exceptionally high, exceeding the 10 parts per billion (ppb) limit set by World Health Organization (WHO 2022), the United States Environmental Protection Agency (USEPA 2022) and the European Union (European Parliament 2020). These results suggest that most of the heavy metals in the

Total number of analyses: 34

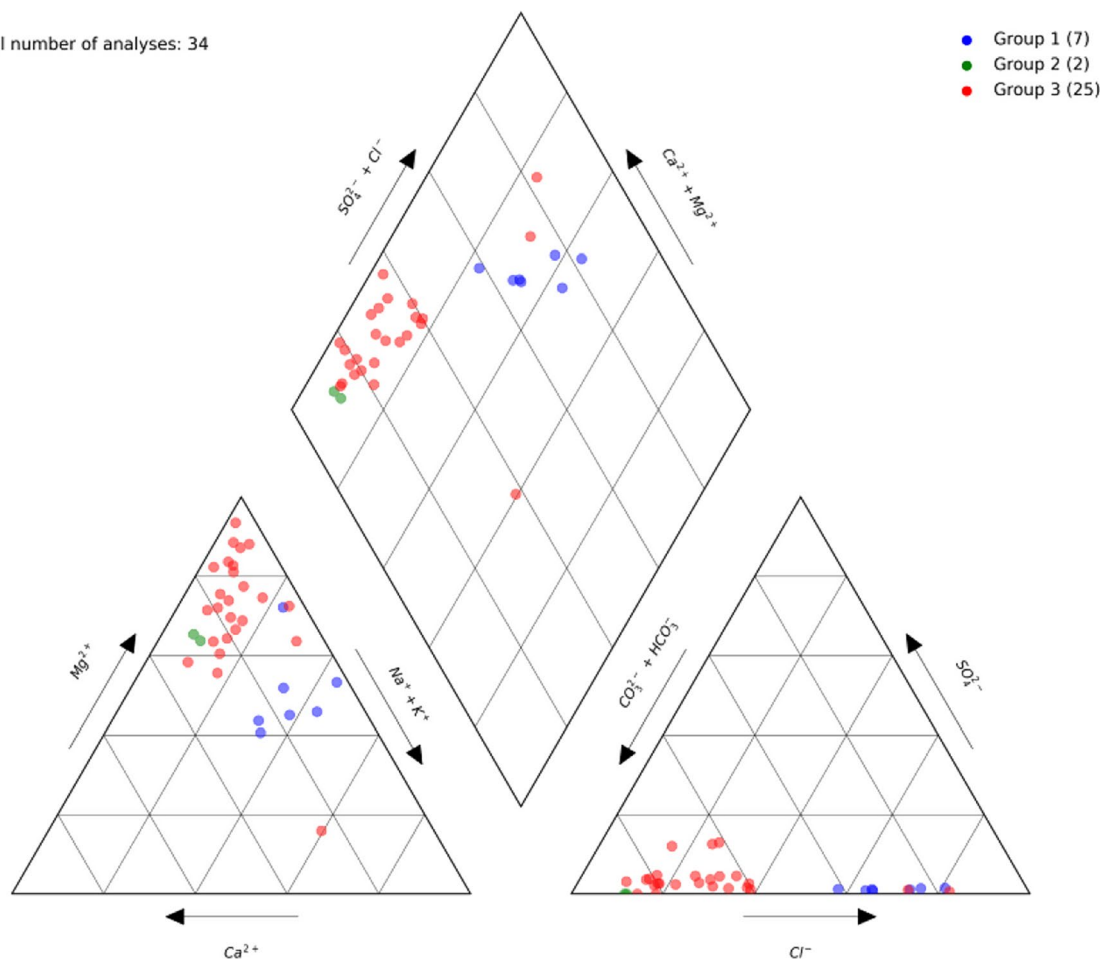


Fig. 3 Piper diagram of water samples collected in three groups of waters (group 1, travertine springs; group 2, surface water; group 3, groundwater) located in Chahar Takab, Fariman county, northeast Iran

Table 2 Pearson correlation coefficients between hydrochemical parameters in waters from Chahar Takab, Fariman county, northeast Iran

	pH	EC	CO ₃ ²⁻	HCO ₃ ⁻	Cl ⁻	SO ₄ ²⁻	Ca ²⁺	Mg ²⁺	Na ⁺	K ⁺
pH	1									
EC	-0.61**	1								
CO ₃ ²⁻	0.38	0.25	1							
HCO ₃ ⁻	-0.81**	0.88**	-0.02	1						
Cl ⁻	-0.59**	0.98**	0.26	0.84**	1					
SO ₄ ²⁻	-0.23	0.63**	0.37*	0.50**	0.62**	1				
Ca ²⁺	-0.70**	0.67**	0.42	0.84**	0.65**	0.38*	1			
Mg ²⁺	-0.62**	0.96**	0.10	0.85**	0.95**	0.58**	0.58**	1		
Na ⁺	-0.57**	0.96**	0.24	0.83**	0.95**	0.61**	0.69**	0.90**	1	
K ⁺	-0.50**	0.95**	0.37*	0.78**	0.94**	0.66**	0.61**	0.87**	0.94**	1

* Significance at the significance level of 0.05

** Significance at the significance level of 0.01

waters are related to travertine springs in the region. However, the occurrence of As in natural waters is related to the water-rock interaction process (Kalender et al. 2015).

Figure 5 illustrates the Metal Index (MI). Results show that 58% of all sampling points have values exceeding one. Group 1 exhibits the highest average MI value (44.99),

surpassing the averages of group 2 (2.38) and group 3 (2.74). Within group 1, CRW3 and CRW4 stands out with exceptionally high MI values of 86.13 and 61.95, respectively. In Group 3, CRW29 is notable for its elevated MI value of 12.41. The contribution of individual metals to the MI calculation in group 1 reveals values exceeding one for

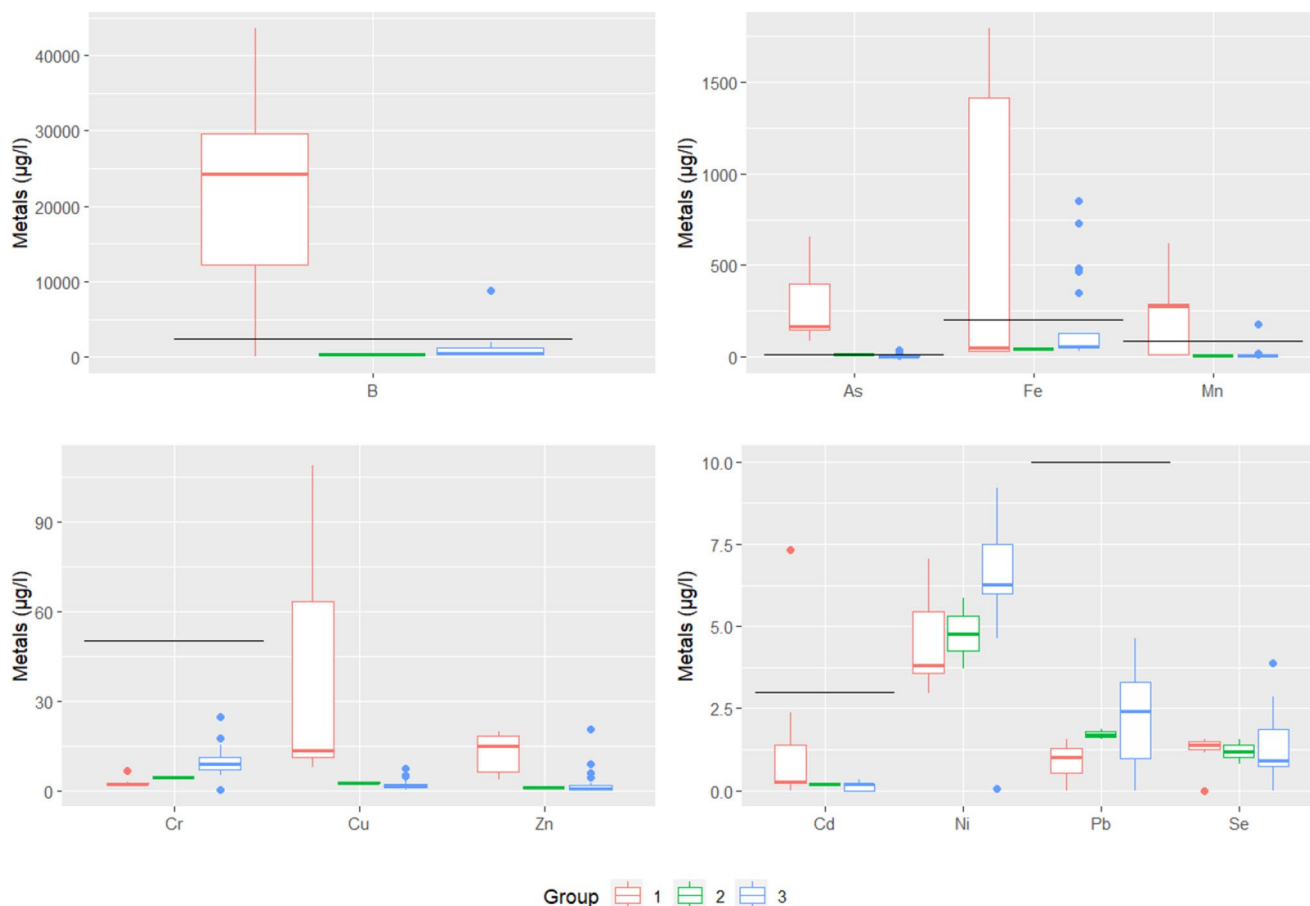


Fig. 4 Concentrations of trace elements in three groups of waters (group 1: travertine springs, red; group 2: surface water, green; group 3: groundwater, blue) located in Chahar Takab, Fariman county, northeast Iran, and comparison with the World Health Organization’s drink-

ing water limits (WHO 2022) indicated by black horizontal lines. If a horizontal line is not present, the limit exceeds the range of the graph or is not defined

As (28.53), B (9.03), Fe (3.40), and Pb (1.21). A summary of non-potable samples and their parameters failing to meet the drinking water standards set by the World Health Organization (2022) and the European Union (2020) is provided in Table 3.

Figure 6 illustrates the proportions of trace-elements-associated risk classes within the 3 groups of water samples according to the guidelines proposed by the United Nations Economic Commission for Europe for the maintenance of aquatic life (UNECE, 1993), as described in Table 4. In summary, samples of group 1 have the highest toxicity risk, with three metals (As, Cd, Pb) having samples classified in class 2 or higher. In contrast, group 3 displays toxic risks for only two elements (Pb and Cd), and group 2 only for one element (Pb). Therefore, Pb shows toxicity in all groups, reaching class 4 in group 1. Cd exhibits toxic associated risks in group 1 and 3, reaching class 4 in group 1. Finally, As shows toxicity risk of class 2 in most of the samples of group 1. Cr, Cu, Ni and Zn fall completely in class 1 in all the groups and therefore, toxicity is not expected.

Beyond the immediate toxicity risks posed by heavy metal-contaminated drinking water, bioaccumulation can increase the risks to humans and other living beings. Some trace elements such As, Cd, Pb, and Hg can cause health problems even at low concentrations (Avigliano et al. 2019; Gupta et al. 2019).

Conclusion

This study highlights the importance of assessing the quality of groundwater, particularly in regions where it serves as a primary water source for human consumption and agricultural purposes. Chahar Takab village in Fariman county, northeast Iran, relies significantly on groundwater, with travertine springs playing a prominent role in the local water supply.

This research reveals the water quality variability of different water sources (travertine springs, surface water, and groundwater) within the study area and key role of

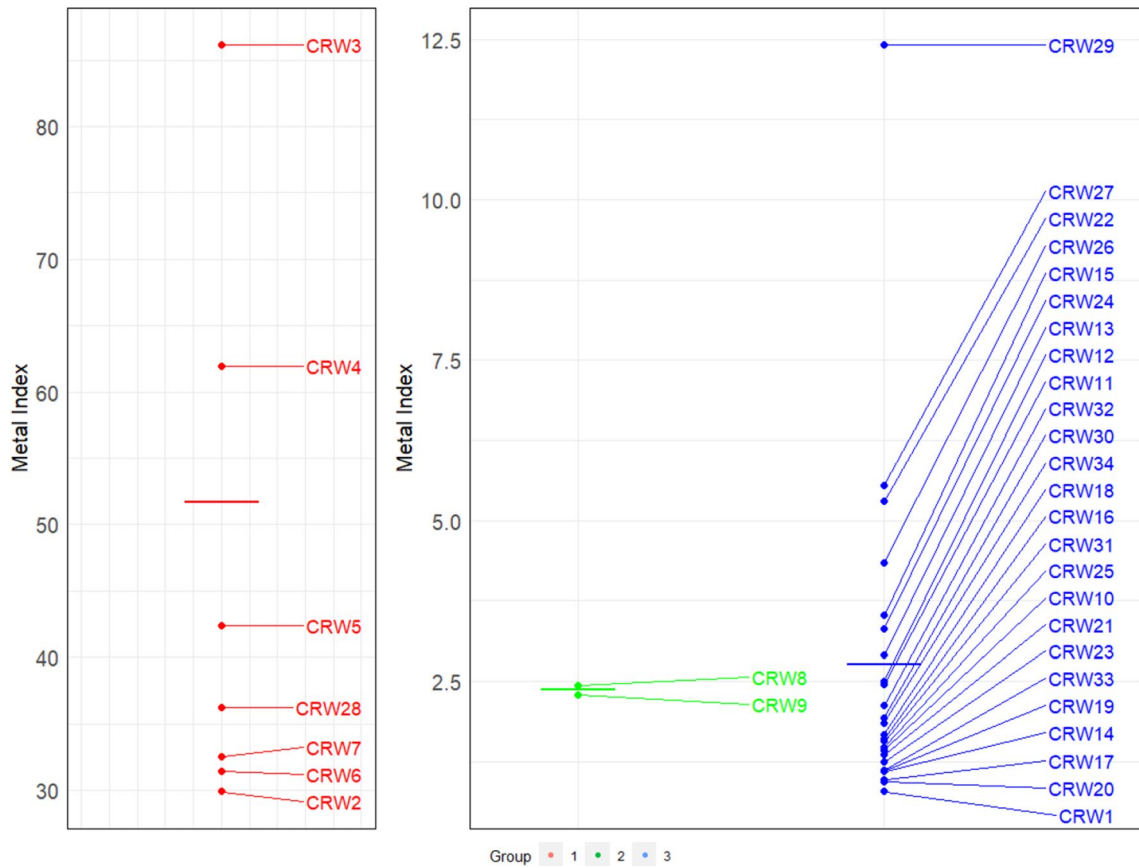


Fig. 5 Metal index values in sampling points across three water groups (group 1: travertine springs, red; group 2: surface water, green; group 3: groundwater, blue) located in Chahar Takab, Fariman county, northeast Iran

Table 3 Non potable samples and parameters exceeding the drinking water limits recommended by the World Health Organization (2022) and the European Union (2020)

Group	Sample ID	Parameter										
Group 1	CRW2	pH	conductivity	Cl-	Na ⁺	As	B			Fe	Mn	
	CRW3	pH	conductivity	Cl-	Na ⁺	As	B			Fe	Mn	
	CRW4	pH	conductivity	Cl-	Na ⁺	As				Fe	Mn	
	CRW5		conductivity	Cl-	Na ⁺	As	B					
	CRW6		conductivity	Cl-	Na ⁺	As	B					
	CRW7		conductivity	Cl-	Na ⁺	As	B					
	CRW28		conductivity	Cl-	Na ⁺	As		Cd	Cu		Pb	
Group 2	CRW8				As							
	CRW9				As							
Group 3	CRW13				As							
	CRW15		conductivity	Cl-	Na ⁺					Fe		
	CRW16				Na ⁺							
	CRW22									Fe		
	CRW24									Fe		
	CRW26									Fe		
	CRW27					As				Fe		
	CRW29					As	B			Fe	Mn	
Permissible limits	WHO (2022)			conductivity	Cl-	Na ⁺						
	European Parliament (2020)	6.5–9.5	2500									

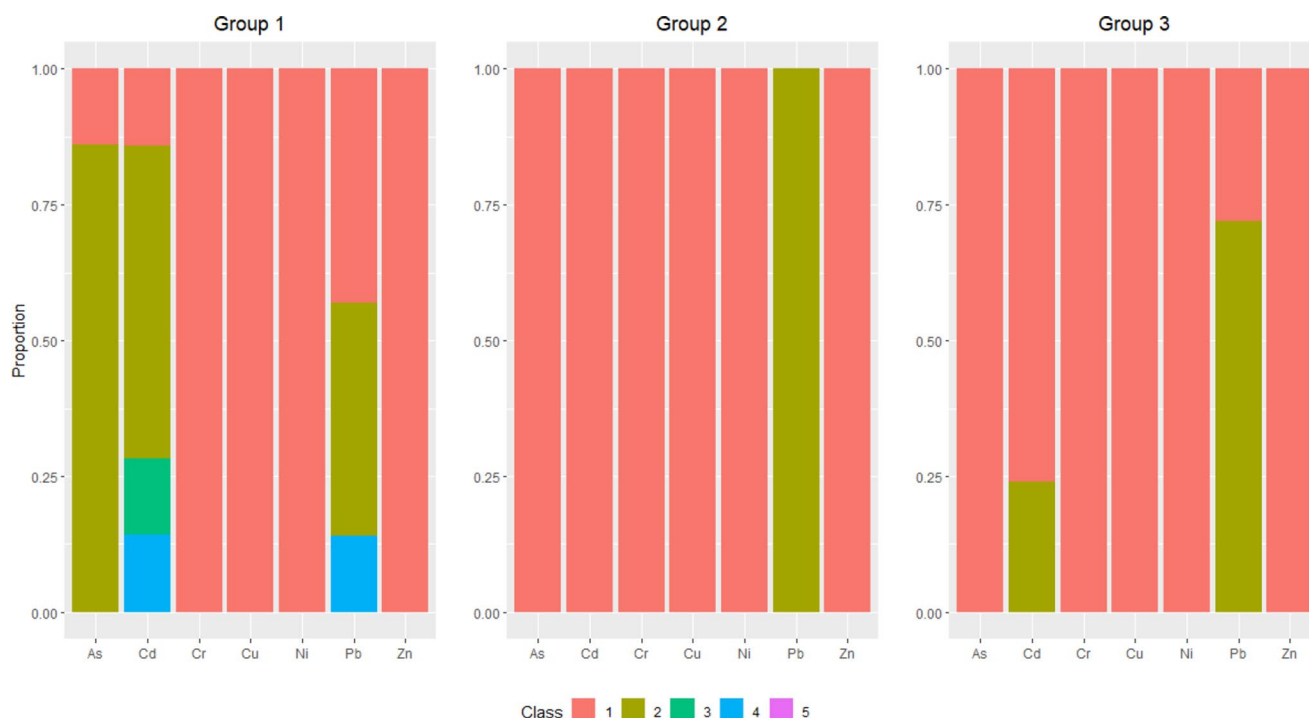


Fig. 6 Proportions of trace-elements-associated risk classes in 3 groups of water samples (group 1: travertine springs; group 2: surface water; group 3: groundwater) collected in Chahar Takab, Fariman county,

Table 4 United Nations Economic Commission for Europe freshwater quality standard ($\mu\text{g/L}$) for the maintenance of aquatic life (UNECE, 1993)

Element	Class I	Class II	Class III	Class IV	Class V
As	<10	10–100	100–190	190–360	>360
Cd	<0.07	0.07–0.53	0.53–1.1	1.1–3.9	>3.9
Cr	<1	1.0–6	6.0–11	11.0–16	>16
Cu	<2	2.0–7	7.0–12	12.0–18	>18
Pb	<0.1	0.1–1.6	1.6–3.2	3.2–82	>82
Hg	<0.003	0.003–0.007	0.007–0.012	0.012–2.4	>2.4
Ni	<15	15–87	87–160	160–1400	>1400
Zn	<45	45–77	77–110	110–120	>120

Interpretation

- Class I: No anthropogenic pollution with inorganic matter
- Class II: Concentrations are below midpoint between natural and chronically toxic levels
- Class III: Concentrations are above midpoint between natural and chronically toxic levels
- Class IV: Excursions beyond chronic criteria occur, but do not establish chronically toxic conditions in terms of concentration levels, duration or frequency
- Class V: Excursions beyond chronic criteria concentrations allow acutely toxic conditions in terms of concentration levels, duration or frequency

travertine springs. When travertine springs were present, results showed lower pH, higher electrical conductivity, and higher concentrations of major ions and heavy metals. Considering World Health Organization guidelines for drinking

northeast Iran following the guideline of UNECE United Nations Economic Commission for Europe (1993)

water, the concentrations of As were especially relevant (exceeded by up to 28.5 times). Other elements such as B, Fe, Mn, and Pb, also exceeded acceptable levels to a lesser extent, while As, Cd, and Pb posed the highest toxicity risks for biota.

Considering these findings, it is recommended that local authorities and stakeholders take action to address water quality issues. This includes conducting regular monitoring of water quality parameters and implementing measures to mitigate heavy metal contamination where necessary. Furthermore, public awareness campaigns and the exploration of alternative water sources may be necessary to ensure the health and well-being of the local population. Further research into the sources and mechanisms of heavy metal contamination in the region is needed to develop effective remediation strategies and safeguard water resources for the future.

Supplementary Information The online version contains supplementary material available at <https://doi.org/10.1007/s12665-025-12144-0>.

Acknowledgements The research was undertaken jointly at Ferdowsi University of Mashhad (FUM), Iran, and Christian Albrechts University of Kiel (CAU), Germany. We are grateful to FUM and CAU for facilitating this research endeavor. Additionally, authors acknowledge financial support from the German Academic Exchange Service (DAAD) through the Indo German Centre for Sustainability (IGCS).

Author contributions M.R.: Conceptualization, Methodology, Validation, Formal analysis, Investigation, Data Curation, Writing - Original Draft, Writing - Review & Editing. M.H.M-G.: Conceptualization, Methodology, Validation, Resources, Writing - Review & Editing, Supervision. N.F.: Resources, Writing - Review & Editing, Supervision. D.R.: Conceptualization, Methodology, Formal analysis, Data Curation, Writing - Original Draft, Visualization, Supervision.

Funding Open Access funding enabled and organized by Projekt DEAL.

Data availability Data is provided within the manuscript or supplementary information files.

Declarations

Competing interests The authors declare no competing interests.

Open Access This article is licensed under a Creative Commons Attribution 4.0 International License, which permits use, sharing, adaptation, distribution and reproduction in any medium or format, as long as you give appropriate credit to the original author(s) and the source, provide a link to the Creative Commons licence, and indicate if changes were made. The images or other third party material in this article are included in the article's Creative Commons licence, unless indicated otherwise in a credit line to the material. If material is not included in the article's Creative Commons licence and your intended use is not permitted by statutory regulation or exceeds the permitted use, you will need to obtain permission directly from the copyright holder. To view a copy of this licence, visit <http://creativecommons.org/licenses/by/4.0/>.

References

- Aju CD, Reghunath R, Achu AL, Rajaneesh A (2022) Understanding the hydrogeochemical processes and physical parameters controlling the groundwater chemistry of a tropical river basin, South India. *Environ Sci Pollut Res* 29:23561–23577. <https://doi.org/10.1007/s11356-021-17455-w>
- Amaral SL, Azevedo LB, Buzalaf MAR, Fabricio MF, Fernandes MS, Valentine RA, Maguire A, Zohoori FV (2018) Effect of chronic exercise on fluoride metabolism in fluorosis-susceptible mice exposed to high fluoride. *Sci Rep* 8:3211. <https://doi.org/10.1038/s41598-018-21616-2>
- American Cancer Society (2020) Arsenic and Cancer Risk [WWW Document]. URL <https://www.cancer.org/healthy/cancer-causes/chemicals/arsenic.html> (accessed 7.3.22)
- Avigliano E, Monferrán MV, Sánchez S, Wunderlin DA, Gastaminza J, Volpedo AV (2019) Distribution and bioaccumulation of 12 trace elements in water, sediment and tissues of the main fishery from different environments of the La Plata basin (South America): risk assessment for human consumption. *Chemosphere* 236:124394. <https://doi.org/10.1016/j.chemosphere.2019.124394>
- Ayotte JD, Belaval M, Olson SA, Burow KR, Flanagan SM, Hinkle SR, Lindsey BD (2015) Factors affecting temporal variability of arsenic in groundwater used for drinking water supply in the United States. *Sci Total Environ* 505:1370–1379. <https://doi.org/10.1016/j.scitotenv.2014.02.057>
- Bhowmick S, Pramanik S, Singh P, Mondal P, Chatterjee D, Nriagu J (2018) Arsenic in groundwater of West Bengal, India: a review of human health risks and assessment of possible intervention options. *Sci Total Environ*. <https://doi.org/10.1016/j.scitotenv.2017.08.216>
- Biswas R, Sarkar A (2019) Characterization of arsenite-oxidizing bacteria to decipher their role in arsenic bioremediation. *Prep Biochem Biotechnol* 49(1):30–37. <https://doi.org/10.1080/10826068.2018.1476883>
- Biswas R, Vivekanand V, Saha A, Ghosh A, Sarkar A (2019) Arsenite oxidation by a facultative chemolithotrophic *Delftia* Spp. *Bas29* for its potential application in groundwater arsenic bioremediation. *Int Biodeterior Biodegrad*. <https://doi.org/10.1016/j.ibiod.2018.10.006>
- Brilli M, Giustini F (2023) Geochemical stratigraphy of the Prima Porta travertine deposit (Roma, Italy). *Minerals* 13:789. <https://doi.org/10.3390/min13060789>
- Chakraborti D, Rahman MM, Ahamed S, Dutta RN, Pati S, Mukherjee SC (2016) Arsenic groundwater contamination and its health effects in Patna district (capital of Bihar) in the middle Ganga plain, India. *Chemosphere* 152:520–529. <https://doi.org/10.1016/j.chemosphere.2016.02.119>
- Delkhabi B, Nassery HR, Vilarrasa V, Alijani F, Ayora C (2020) Impacts of natural CO₂ leakage on groundwater chemistry of aquifers from the Hamadan Province, Iran. *Int J Greenh Gas Control* 96:103001. <https://doi.org/10.1016/j.ijggc.2020.103001>
- Durowoju O, Odiyo J, Ekosse GI (2015) Hydrogeochemical setting of geothermal springs in Limpopo Province, South Africa. *Res J Chem Environ* 19:77–88
- European Parliament (2020) Directive (EU) 2020/2184 of the European Parliament and of the Council of 16 December 2020 on the quality of water intended for human consumption [WWW Document]. URL <https://eur-lex.europa.eu/eli/dir/2020/2184/oj> (accessed 6.8.22)
- Foster SA, Pennino MJ, Compton JE, Leibowitz SG, Kile ML (2019) Arsenic drinking water violations decreased across the United States following revision of the Maximum Contaminant Level. *Environ Sci Technol* 53:11478–11485. <https://doi.org/10.1021/acs.est.9b02358>
- Gao W, Zhang J, Sun D, Zhang W, Wang S, Guo J, Xu H, Zhao S, Zeng Y, Liu X (2023) Water Environmental characteristics and eutrophication evaluation of Alpine Karst Mountains in Huanglong, Sichuan, China. *ACS Earth Sp Chem* 7:1083–1096. <https://doi.org/10.1021/acsearthspacechem.3c00015>
- Ghosh S, Majumder S, Roychowdhury T (2019) Assessment of the effect of urban pollution on surface water-groundwater system of Adi Ganga, a historical outlet of river Ganga. *Chemosphere* 237:124507. <https://doi.org/10.1016/j.chemosphere.2019.124507>
- Grootjans A, Bulte M, Wolejko L, Pakalne M, Dullo B, Eck N, Fritz C (2015) Prospects of damaged calcareous spring systems in temperate Europe: can we restore travertine-marl deposition? *Folia Geobot* 50:1–11. <https://doi.org/10.1007/s12224-015-9214-z>
- Guettaf M, Maoui A, Ihdene Z (2017) Assessment of water quality: a case study of the Seybouse River (North East of Algeria). *Appl Water Sci* 7:295–307. <https://doi.org/10.1007/s13201-014-0245-z>
- Gupta N, Yadav KK, Kumar V, Kumar S, Chadd RP, Kumar A (2019) Trace elements in soil-vegetables interface: translocation, bioaccumulation, toxicity and amelioration - A review. *Sci Total Environ* 651:2927–2942. <https://doi.org/10.1016/j.scitotenv.2018.10.047>
- Hamidian AH, Razezghi N, Zhang Y, Yang M (2019) Spatial distribution of arsenic in groundwater of Iran, a review. *J Geochemical Explor* 88–98. <https://doi.org/10.1016/j.gexplo.2019.03.014>
- He S, Wu J (2019a) Hydrogeochemical Characteristics, Groundwater Quality, and Health risks from Hexavalent Chromium and Nitrate in Groundwater of Huanhe formation in Wuqi County, Northwest China. *Expo Heal* 11:125–137. <https://doi.org/10.1007/s12403-018-0289-7>

- He S, Wu J (2019b) Relationships of groundwater quality and associated health risks with land use/land cover patterns: a case study in a loess area, Northwest China. *Hum Ecol Risk Assess Int J* 25:354–373. <https://doi.org/10.1080/10807039.2019.1570463>
- He X, Li P, Ji Y, Wang Y, Su Z, Elumalai V (2020) Groundwater Arsenic and Fluoride and Associated Arsenicosis and Fluorosis in China: occurrence, distribution and management. *Expo Heal* 12:355–368. <https://doi.org/10.1007/s12403-020-00347-8>
- Henchiri M, Ben Ahmed W, Brogi A, Alçiçek MC, Benassi R (2017) Evolution of pleistocene travertine depositional system from terraced slope to fissure-ridge in a mixed travertine-alluvial succession (Jebel El Mida, Gafsa, Southern Tunisia). *Geodin Acta* 29:20–41. <https://doi.org/10.1080/09853111.2016.1265398>
- Hiett CD, Newell DL, Jessup MJ, Grambling TA, Scott BE, Upin HE (2022) Deep CO₂ and N₂ emissions from Peruvian Hot Springs: stable isotopic constraints on volatile cycling in a flat-slab subduction zone. *Chem Geol* 595:120787
- Hossain S, Hosono T, Ide K, Matsunaga M, Shimada J (2016) Redox processes and occurrence of arsenic in a volcanic aquifer system of Kumamoto Area. *Japan Environ Earth Sci* 75:740. <https://doi.org/10.1007/s12665-016-5557-x>
- Hounslow AW (2018) Water quality data: analysis and interpretation, First. Ed, Water Quality Data: analysis and interpretation. CRC, Boca Raton, FL, USA. <https://doi.org/10.1201/9780203734117>
- Huq ME, Fahad S, Shao Z, Sarven MS, Khan IA, Alam M, Saeed M, Ullah H, Adnan M, Saud S, Cheng Q, Ali S, Wahid F, Zamin M, Raza MA, Saeed B, Riaz M, Khan WU (2020) Arsenic in a groundwater environment in Bangladesh: occurrence and mobilization. *J Environ Manage* 262:110318. <https://doi.org/10.1016/j.jenvman.2020.110318>
- IPCC (2022) Sixth Assessment Report Fact sheet - Food and Water
- Iran Data Portal (2022) Iran Meteorological Organization [WWW Document]. URL <https://irandataportal.syrr.edu/iran-meteorological-organization> (accessed 3.18.22)
- Iran Oil, Company (1957) Geological Map of Iran [WWW Document]. URL <https://esdac.jrc.ec.europa.eu/content/geological-map-iran> (accessed 8.28.23)
- Islam MS (2023) Introduction to Hydrogeochemical Processes, in: Islam, M.S. (Ed.), Hydrogeochemical Evaluation and Groundwater Quality. Springer. https://doi.org/10.1007/978-3-031-44304-6_1
- Janssens N, Capezzuoli E, Claes H, Muchez P, Yu TL, Shen CC, Ellam RM, Swennen R (2020) Fossil travertine system and its palaeofluid provenance, migration and evolution through time: Example from the geothermal area of Acquasanta Terme (Central Italy). *Sediment Geol* 398:105580. <https://doi.org/10.1016/j.sedgeo.2019.105580>
- Kalender L, Öztekin Okan Ö, Inceöz M, Çetindağ B, Yildirim V (2015) Geochemistry of travertine deposits in the eastern Anatolia district: an example of the karakoçan-yoğunağaç (elazığ) and mazgirt-dedebağ (tunceli) travertines, Turkey. *Turkish J Earth Sci* 24:607–626. <https://doi.org/10.3906/yer-1504-27>
- Kampouroglou EE, Economou-Eliopoulos M (2016) Assessment of the environmental impact by as and heavy metals in lacustrine travertine limestone and soil in Attica, Greece: mapping of potentially contaminated sites. *CATENA* 139:137–166. <https://doi.org/10.1016/j.catena.2015.12.009>
- Kano A, Okumura T, Takashima C, Shiraishi F (2019) Geomicrobiological Properties and processes of Travertine, Springer Geology. Springer Singapore, Singapore. <https://doi.org/10.1007/978-981-13-1337-0>
- Kele S, Bódai B (2022) Age, Depositional Environment, and Geochemistry of Freshwater Carbonates (Travertine, Tufa) from Hungary. In: Veress M, Leél-Össy S (eds) Cave and Karst systems of Hungary. Cave and Karst Systems of the World. Springer
- Kumar R, Patel M, Singh P, Bundschuh J, Pittman CU, Trakal L, Mohan D (2019) Emerging technologies for arsenic removal from drinking water in rural and peri-urban areas: methods, experience from, and options for Latin America. *Sci Total Environ* 694:133427. <https://doi.org/10.1016/j.scitotenv.2019.07.233>
- Luo L, Capezzuoli E, Rogerson M, Vaselli O, Wen H, Lu Z (2022) Precipitation of carbonate minerals in travertine-depositing Hot Springs: driving forces, microenvironments, and mechanisms. *Sediment Geol* 438:106207. <https://doi.org/10.1016/j.sedgeo.2022.106207>
- Masoudinejad M, Ghaderpoori M, Zarei A, Nasehifar J, Malekzadeh A, Nasiri J, Ghaderpoury A (2018) Data on phosphorus concentration of rivers feeding into Taham dam in Zanjan, Iran. *Data Br* 17:564–569. <https://doi.org/10.1016/j.dib.2018.01.068>
- Mohammadzadeh H, Daneshvar M, M.R (2020) A comparison of hydro-geochemistry and stable isotope composition of travertine-depositing springs, Garab in NE Iran and Pamukkale in SW Turkey. *Carbonates Evaporites* 35:23. <https://doi.org/10.1007/s13146-020-00566-9>
- Moreno Merino L, Aguilera H, González-Jiménez M, Díaz-Losada E (2021) D-Piper, a modified piper diagram to represent big sets of hydrochemical analyses. *Environ Model Softw* 138:104979. <https://doi.org/10.1016/j.envsoft.2021.104979>
- Mueller B (2017) Arsenic in groundwater in the southern lowlands of Nepal and its mitigation options: a review. *Environ Rev* 25:296–305. <https://doi.org/10.1139/er-2016-0068>
- Nugraheni RD, Sunjaya D (2019) Geochemical Approach to reveal the Genetic Occurrence of Gibbsite, relative to the parent rock type in Lateritic bauxites. *J Phys Conf Ser* 1363:012042. <https://doi.org/10.1088/1742-6596/1363/1/012042>
- Ortega-Guerrero A (2017) Evaporative concentration of arsenic in groundwater: health and environmental implications, La Laguna Region. *Mexico Environ Geochem Health* 39:987–1003. <https://doi.org/10.1007/s10653-016-9866-5>
- Pazhoor MT, Gautam PK, Samanta S, Suman, Bangotra P, Banerjee S (2021) Performance assessment of Zn–Sn bimetal oxides for the removal of inorganic arsenic in groundwater. *Groundw Sustain Dev* 14:100600. <https://doi.org/10.1016/j.gsd.2021.100600>
- Piper AM (1944) A graphic procedure in the geochemical interpretation of water-analyses. *Eos Trans Am Geophys Union* 25:914–928. <https://doi.org/10.1029/TR025I006P00914>
- Pola M, Gandin A, Tuccimei P, Soligo M, Deiana R, Fabbri P, Zampieri D (2014) A multidisciplinary approach to understanding carbonate deposition under tectonically controlled hydrothermal circulation: a case study from a recent travertine mound in the Euganean hydrothermal system, northern Italy. *Sedimentology* 61:172–199. <https://doi.org/10.1111/sed.12069>
- Pollastro R, Persits F, Steinshouer DW (1999) Surficial geology of Iran (geo2cg) [WWW Document]. U.S. Geol. Surv. data release. <https://doi.org/10.5066/P93ZEPFY> (accessed 1.10.25)
- Ranjbaran M, Zamanzadeh SM (2021) Determining the role of chemical and biological factors in controlling precipitation of tufa and travertine deposits in Shurab area, Northern Iran. *Carbonates Evaporites* 36:73. <https://doi.org/10.1007/s13146-021-00691-z>
- Rezaei A, Hassani H, Hayati M, Jabbari N, Barzegar R (2018) Risk assessment and ranking of heavy metals concentration in Iran's Rayen groundwater basin using linear assignment method. *Stoch Environ Res Risk Assess* 32:1317–1336. <https://doi.org/10.1007/s00477-017-1477-x>
- Roh T, Lynch CF, Weyer P, Wang K, Kelly KM, Ludewig G (2017) Low-level arsenic exposure from drinking water is associated with prostate cancer in Iowa. *Environ Res* 159:338–343. <https://doi.org/10.1016/j.envres.2017.08.026>
- Shakeri A, Sharifi Fard M, Mehrabi B, Rastegari Mehr M (2020) Occurrence, origin and health risk of arsenic and potentially toxic elements (PTEs) in sediments and fish tissues from the

- geothermal area of the Khiav River, Ardebil Province (NW Iran). *J Geochemical Explor* 106347. <https://doi.org/10.1016/j.gexplo.2019.106347>
- Shakoor MB, Bibi I, Niazi NK, Shahid M, Nawaz MF, Farooqi A, Naidu R, Rahman MM, Murtaza G, Lüttge A (2018) The evaluation of arsenic contamination potential, speciation and hydrogeochemical behaviour in aquifers of Punjab. *Pakistan Chemosphere* 199:737–746. <https://doi.org/10.1016/j.chemosphere.2018.02.002>
- Shiraishi F, Morikawa A, Kuroshima K, Amekawa S, Yu TL, Shen CC, Kakizaki Y, Kano A, Asada J, Bahniuk AM (2020) Genesis and diagenesis of travertine, Futamata hot spring. *Japan Sediment Geol* 405:105706. <https://doi.org/10.1016/j.sedgeo.2020.105706>
- Tamasi G, Cini R (2004) Heavy metals in drinking waters from Mount Amiata (Tuscany, Italy). Possible risks from arsenic for public health in the Province of Siena. *Sci Total Environ* 327:41–51. <https://doi.org/10.1016/j.scitotenv.2003.10.011>
- Tapia J, Murray J, Ormachea M, Tirado N, Nordstrom DK (2019) Origin, distribution, and geochemistry of arsenic in the Altiplano-Puna plateau of Argentina, Bolivia, Chile, and Perú. *Sci Total Environ* 678:309–325. <https://doi.org/10.1016/j.scitotenv.2019.04.084>
- Ulloa-Cedamano F, Probst JL, Binet S, Camboulive T, Payre-Suc V, Pautot C, Bakalowicz M, Beranger S, Probst A (2020) A forty-year karstic critical zone survey (Baget Catchment, Pyrenees-France): Lithologic and hydroclimatic controls on Seasonal and Inter-annual Variations of Stream Water Chemical Composition, pCO₂, and Carbonate Equilibrium. *Water* 2020(12):Page122712–Page121227. <https://doi.org/10.3390/W12051227>
- UNECE United Nations Economic Commission for Europe (1993) Standard Statistical Classification of Surface Freshwater Quality for the maintenance of aquatic life. Readings in International Environment statistics. United Nations Economic Commission for Europe, United Nations, New York and Geneva, p 546
- UNESCO World Water Assessment Programme (2022) The United Nations World Water Development Report 2022: groundwater: making the invisible visible
- United Nations (2022) The Sustainable Development Goals Report 2022
- USEPA (2023) National Recommended Water Quality Criteria - Aquatic Life Criteria Table [WWW Document]. URL <https://www.epa.gov/wqc/national-recommended-water-quality-criteria-aquatic-life-criteria-table> (accessed 7.17.23)
- USEPA (2022) Table of Secondary Standards. Secondary Drinking Water Standards: Guidance for Nuisance Chemicals [WWW Document]. URL <https://www.epa.gov/sdwa/secondary-drinking-water-standards-guidance-nuisance-chemicals> (accessed 5.10.22)
- USEPA (2004) Evaluation of the potential carcinogenicity of arsenic compounds [WWW Document]. URL https://cfpub.epa.gov/si/si_public_record_Report.cfm?Lab=ORD&dirEntryID=41925 (accessed 7.3.22)
- Vardhan KH, Kumar PS, Panda RC (2019) A review on heavy metal pollution, toxicity and remedial measures: current trends and future perspectives. *J Mol Liq*. <https://doi.org/10.1016/j.molliq.2019.111197>
- Wang X, Zhou X, Zhao J, Zheng Y, Song C, Long M, Chen T (2015) Hydrochemical evolution and reaction simulation of travertine deposition of the Lianchangping Hot Springs in Yunnan, China. *Quat Int* 374:62–75. <https://doi.org/10.1016/j.quaint.2014.09.046>
- WHO (2022) Guidelines for drinking-water quality, 4th edition, incorporating the 1st and 2nd addenda. Geneva
- WHO (2005) Nutrients in Drinking Water
- World Bank (2021) Climate change knowledge portal [WWW Document]. URL <https://climateknowledgeportal.worldbank.org/country/iran-islamic-rep> (accessed 8.31.22)
- World Meteorological Organization (2022) Protect our people and future generations: Water and Climate Leaders call for urgent action [WWW Document]. URL <https://public.wmo.int/en/media/press-release/protect-our-people-and-future-generations-water-and-climate-leaders-call-urgent> (accessed 3.18.23)
- Yousefi M, Dehghani MH, Nasab SM, Taghavimanesh V, Nazmara S, Mohammadi AA (2018) Data on trend changes of drinking groundwater resources quality: a case study in Abhar. *Data Br* 17:424–430. <https://doi.org/10.1016/J.DIB.2018.01.032>
- Zhang Y, Zhou X, Liu H, Hai K, Yu M, Tan M (2020) Characterization of a saline hot spring depositing travertine in the red beds in the Simao Basin of China. *Hydrogeol J* 28:1431–1447. <https://doi.org/10.1007/s10040-020-02126-w>

Publisher's note Springer Nature remains neutral with regard to jurisdictional claims in published maps and institutional affiliations.